



## OPEN ACCESS

## EDITED BY

Jin Zhou,  
Tsinghua University, China

## REVIEWED BY

Drishiti Kaul,  
J. Craig Venter Institute, United States  
Paraskevi Mara,  
Woods Hole Oceanographic Institution,  
United States

## \*CORRESPONDENCE

Stefan Thiele  
✉ stefan.thiele@uib.no

RECEIVED 28 April 2023

ACCEPTED 15 June 2023

PUBLISHED 07 July 2023

## CITATION

Thiele S, Vader A, Thomson S, Saubrekka K, Petelenz E, Müller O, Bratbak G and Øvreås L (2023) Seasonality of the bacterial and archaeal community composition of the Northern Barents Sea. *Front. Microbiol.* 14:1213718. doi: 10.3389/fmicb.2023.1213718

## COPYRIGHT

© 2023 Thiele, Vader, Thomson, Saubrekka, Petelenz, Müller, Bratbak and Øvreås. This is an open-access article distributed under the terms of the [Creative Commons Attribution License \(CC BY\)](https://creativecommons.org/licenses/by/4.0/). The use, distribution or reproduction in other forums is permitted, provided the original author(s) and the copyright owner(s) are credited and that the original publication in this journal is cited, in accordance with accepted academic practice. No use, distribution or reproduction is permitted which does not comply with these terms.

# Seasonality of the bacterial and archaeal community composition of the Northern Barents Sea

Stefan Thiele<sup>1,2\*</sup>, Anna Vader<sup>3</sup>, Stuart Thomson<sup>3</sup>,  
Karoline Saubrekka<sup>4</sup>, Elzbieta Petelenz<sup>1</sup>, Oliver Müller<sup>1</sup>,  
Gunnar Bratbak<sup>1</sup> and Lise Øvreås<sup>1,3</sup>

<sup>1</sup>Department of Biological Science, University of Bergen, Bergen, Norway, <sup>2</sup>Bjerknes Centre for Climate Research, Bergen, Norway, <sup>3</sup>University Center in Svalbard (UNIS), Longyearbyen, Norway, <sup>4</sup>Department of Bioscience, University of Oslo, Oslo, Norway

The Barents Sea is a transition zone between the Atlantic and the Arctic Ocean. The ecosystem in this region is highly variable, and a seasonal baseline of biological factors is needed to monitor the effects of global warming. In this study, we report the results from the investigations of the bacterial and archaeal community in late winter, spring, summer, and early winter along a transect through the northern Barents Sea into the Arctic Ocean east of Svalbard using 16S rRNA metabarcoding. Winter samples were dominated by members of the SAR11 clade and a community of nitrifiers, namely *Cand. Nitrosopumilus* and LS-NOB (*Nitrospina*), suggest a prevalence of chemoautotrophic metabolisms. During spring and summer, members of the *Gammaproteobacteria* (mainly members of the SAR92 and OM60(NOR5) clades, *Nitrospiraceae*) and *Bacteroidia* (mainly *Polaribacter*, *Formosa*, and members of the NS9 marine group), which followed a succession based on their utilization of different phytoplankton-derived carbon sources, prevailed. Our results indicate that Arctic marine bacterial and archaeal communities switch from carbon cycling in spring and summer to nitrogen cycling in winter and provide a seasonal baseline to study the changes in these processes in response to the effects of climate change.

## KEYWORDS

microbial ecology, Arctic, the Nansen Legacy, polar microbes, carbon cycling, nitrogen cycling

## 1. Introduction

As an effect of global warming, the Arctic warms four times faster than the global average (Rantanen et al., 2022). In the Arctic, the Barents Sea is a transition zone between the Atlantic and the Arctic Ocean. In this study, warm Atlantic water mixes with cold Arctic water over a shallow shelf area. In the northern Barents Sea, the effects of the influx of Atlantic water masses are, among others, increased productivity and the potential influx of phytoplankton blooms (Ingvaldsen et al., 2021), which may have profound effects on the highly dynamic marine ecosystems of the Arctic (Loeng, 1991; Reigstad et al., 2002; Wassmann et al., 2011; Smedsrud et al., 2013). Seasonal changes between the dark winter and the light summer are extreme, and the harsh environmental conditions during winter have made most sampling campaigns in the Arctic focused on the light season. Due to its high variability,

seasonal baselines for the biological components of the ecosystem are necessary to investigate changes and predict the consequences of global warming. The aim of the Nansen Legacy project is to provide such a baseline in a holistic approach, including the microbial loop and the bacterial and archaeal communities.

During spring, phytoplankton blooms occur, and the primary production increases in the open water and under the sea ice in the Barents Sea and the Arctic Ocean (Sakshaug, 2004; Hodal and Kristiansen, 2008; Ardyna et al., 2020). Such spring blooms are the main source of carbon in marine ecosystems and vary in strength depending on freshwater influx due to sea ice melt in the Northern Barents Sea (Hunt et al., 2013; Silva et al., 2021). These blooms are followed by successions of mostly heterotrophic bacteria such as *Bacteroidia*, *Gammaproteobacteria*, and *Alphaproteobacteria* (*Rhodobacteraceae*), based on the predominant carbon sources (Teeling et al., 2012, 2016; de Sousa et al., 2019; Wietz et al., 2021; Thiele et al., 2023). Therefore, during summer, the communities are dominated by *Gammaproteobacteria* (*Nitrincolaceae*, members of the SAR92 and OM60(NOR5) clades, *Halomonadaceae*, *Pseudohongiellaceae*, and *Alteromonadaceae*), *Bacteroidetes* (*Polaribacter*, *Formosa*, and *Ulvibacter*), and *Alphaproteobacteria* (members of the SAR11 clades, *Rhodobacteraceae*, and *Roseobacter*). The exploitation of phytoplankton-derived carbon remains dominant until autumn with different bacterial groups, e.g., *Flavobacteriaceae* and *Rhodobacteraceae*, dominating the carbon decomposition at different times. Other groups, such as *Nitrosphaerota* (*Candidatus Nitrosopumilus*), *Marinimicrobia* (SAR406 clade), and *Chloroflexi* (members of the SAR202 clade), are abundant in sub-seasurface waters during all seasons (Alonso-Sáez et al., 2012; Grzymiski et al., 2012; Wilson et al., 2017; Müller et al., 2018; Wietz et al., 2021; Thiele et al., 2023). During the winter months, ammonia oxidation by *Nitrosphaerota* (formerly associated with *Thaumarchaea*), namely *Cand. Nitrosopumilus* becomes a major metabolic process in the surface and sub-seasurface waters. This results in the replenishment of the nitrate concentrations in surface waters, where it is taken up by the phytoplankton in spring (Grzymiski et al., 2012; Connelly et al., 2014).

In this study, we present an investigation of the bacterial and archaeal community of a transect from the northern Barents Sea into the Arctic Ocean during late winter, spring, summer, and early winter setting a baseline for future investigations with regard to global warming-induced changes and their effect on the microbial community.

## 2. Materials and methods

### 2.1. Sampling and environmental parameters

Samples were collected during four seasonal sampling campaigns on the RV “Kronprins Haakon,” during different quarters (Q) of the year along the standard transect of the Nansen Legacy project in the northern Barents Sea east of Svalbard

(stations P1–P7; Figure 1): Q3 (cruise 2019706) from 6 to 23 August 2019, Q4 (cruise 2019711) from 28 November to 17 December 2019, Q1 (cruise 2021703) from 2 to 24 March 2021, and Q2 (cruise 2021704) from 27 April to 20 May 2021, with Q1 representing “late winter,” Q2 “spring,” Q3 “summer,” and Q4 “early winter.” The stations were chosen to cover several factors of the Northern Barents Sea, such as Atlantic water influence (P1, P6, and P7), possible sea ice coverage (P5–P7), the Barents Sea shelf (P1–P5), the shelf break (P6), and the Arctic Basin (P7). All samples were taken as single samples using a Niskin rosette following the latest version of the Nansen Legacy protocol (The Nansen Legacy, 2021). Samples for the analyses of the bacterial and archaeal communities were collected at 10 m, the chlorophyll *a* max, or 20 m if no chlorophyll *a* max was found, 200 m, 1,000 m when possible, and 10 m above the sea floor. The differences in depth are due to slight differences in the sea floor depth around the station, which in combination with the CTD depth, drift, and other parameters during sampling leads to slight variation, especially at the deeper stations. Samples deeper than 50 m were defined as “sub-seasurface” based on the differences in the community composition compared to surface samples (0–50 m). All water samples were filtered using 0.22  $\mu\text{m}$  Sterivex filters (Merck, Darmstadt, Germany), frozen immediately, and kept at  $-80^{\circ}\text{C}$  until DNA extraction. During sampling campaigns, temperature, salinity, and the concentrations of phosphate, silicate, nitrate, and nitrite were measured (Chierici, 2021a,b; Jones et al., 2022a,b). In addition, the sea ice coverage and the days without ice cover were noted (Steer and Divine, 2023). Chl *a* concentrations were measured using a Turner Design Fluorometer from seawater after extraction from GFF filters using methanol. Bacterial and archaeal cell numbers were determined using a FACSCalibur (Becton Dickinson, Franklin Lake, US) flow cytometer according to Brussaard and co-workers (Marie et al., 1999; Brussaard, 2004). Aliquots of 100  $\mu\text{m}$  were taken from 1.8 ml of glutaraldehyde-fixed seawater samples and diluted to concentrations expected to yield the most accurate flow cytometry counts. The dilutions were stained using SYBR Green I DNA dye and counted at a low flow rate of  $\sim 60 \mu\text{l min}^{-1}$  using a bi-parametric plot of green fluorescence (530/30) vs. side scatter (SSC,488/10) to differentiate cells. All samples are presented as numbers with standard errors.

### 2.2. DNA extraction and sequencing

DNA extractions were performed using the DNeasy Power Water Sterivex Kit (QIAGEN, Hilden, Germany) according to the manual. The extracted DNA was used for sequencing library construction, targeting the V4 region of the 16S rRNA genes of the bacterial and archaeal communities, using primers 515F–5′-GTGYCAGCMGCCGCGGTAA-3′ and 806R–5′-GGACTACNVGGGTWTCTAAT-3′ (Apprill et al., 2015; Parada et al., 2016). The libraries were sequenced using Illumina MiSeq technology with paired-end reads of  $2 \times 250$  bp length at the Integrated Microbiome Resource in Halifax, Canada. The raw reads were deposited in the European Nucleotide Archive as project PRJEB57296.

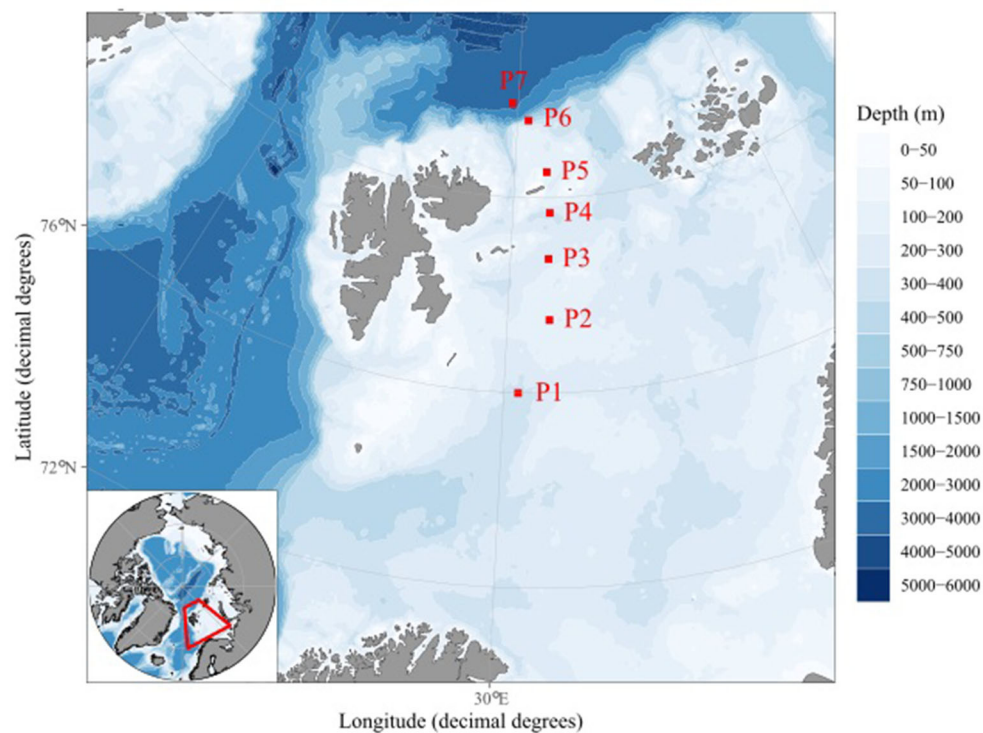


**FIGURE 1**  
Map of the Nansen Legacy transect in the Barents Sea with stations P1 to P7 marked in red. The map was made using “ggOceanMaps” (Vihtakari, 2022).

## 2.3. Sequence analyses

The DADA2 pipeline was used in R to generate Amplicon sequence variants (ASVs) (Callahan et al., 2016). For this, primers were removed, the quality of the sequences was checked, and a static trim with 230 bp and 200 bp was conducted. The final ASVs were then generated after dereplication. Subsequently, the complementary reads were merged, chimeras were removed, and the taxonomy was assigned to the ASVs using a trained Silva database, based on the Silva release SSU Ref NR v138 (Quast et al., 2013). Thereafter, ASVs identified as mitochondria, chloroplasts, eukaryotes, <4 sequences or <  $1 \times 10^{-5}\%$  of relative abundance, as well as samples with <10,000 reads were removed (Supplementary material 1). The samples are presented with relative abundances with standard deviations if applicable.

All analyses were performed using R in RStudio (R Core Team, 2021) with the packages “tidyverse,” “phyloseq” for the analyses of the community data (McMurdie and Holmes, 2013; Wickham et al., 2019) and “ape” and “forcats” as supportive packages (Paradis and Schliep, 2019; Wickham, 2020). Visualizations were performed using the packages “ggplot2,” “scales,” and “patchwork” (Wickham, 2009; Lin Pedersen, 2020; Wickham and Seidel, 2020), while statistics were performed using the “vegan” and “mixOmics” packages (Rohart et al., 2017; Oksanen et al., 2020). An approximate maximum likelihood tree was calculated using FastTree2 (Price et al., 2010) based on alignments using the SINA aligner (Pruesse et al., 2012). A redundancy analysis (RDA) including an ANOVA

test for the significance of different factors was conducted using “microbiomeSeq” (Ssekagiri et al., 2017). In addition, a partial least square regression (PLSR) analysis was performed using the “mixOmics” package (Rohart et al., 2017). Using PiCRUST2 with standard parameters in bioconda, the metabolic potential of the different ASVs was inferred based on their location in a phylogenetic tree of fully sequenced organisms and the genomic assets of the closest relative in this tree (Grüning et al., 2018; Douglas et al., 2020). Using enzyme commission (EC)-numbers, the carbohydrate-active enzymes (CAZymes) belonging to the classes of auxiliary activities (AAs), glycoside hydrolases (GH), polysaccharide lyases (PL), carbohydrate esterases (CE), carbohydrate-binding modules (CBMs), and glycosyltransferase (GT) were extracted. CAZymes classified as GH and CBM were merged into GH. Similarly, marker genes, namely *nifH*, *nirS/nirK*, *norB*, *nosZ*, *narB*, *hzsA*, *amoA-pmoA*, *hao*, *nrfA*, *aprA*, *dsrA*, *cysH*, *soxB*, *mmoX*, *mcrA*, *psaA*, and *psbA* were used for the analyses (Supplementary materials 2, 3).

## 3. Results

### 3.1. Environmental variables

In early and late winter, as well as in spring, stations P2–P7 were ice covered, while in summer P4–P7 were covered. The ice cover ranged between 80 and 100% coverage. Station P1 was

ice-free for 268 days in late winter, 324 days in spring, and 215 days in early winter. In summer, stations P1–P3 were ice-free for 89, 43, and 44 days, respectively. The salinity ranged  $\sim 34.5 \pm 0.4$  PSU, indicating the presence of polar water and warm polar water (Sundfjord et al., 2020). Lower salinities were measured on the surface of ice-covered stations, especially during summer and early winter, with the lowest value of 32.0 PSU recorded at 10 m depth at P5 during summer (Supplementary Figure 1 and Supplementary material 4). Thus, salinity is a significant (ANOVA;  $p = 0.001$ ) factor explaining the bacterial and archaeal community composition on the surface, separating the summer from the rest of the seasons, as well as P6 and P7 from the other stations in the sub-seasurface (Figure 2). This separation is intensified by the differences in temperature (ANOVA;  $p = 0.001$ ; Figure 2). Temperatures ranged from a maximum value of  $4.72^\circ\text{C}$  at 6 m at the southernmost station P1 during summer to  $-1.87^\circ\text{C}$  at most depths at P3 during early winter (Supplementary Figure 1 and Supplementary material 4). Generally, temperatures were lower in surface waters than in the sub-seasurface, especially in ice-covered stations (Supplementary Figure 1).

Phosphate, silicate, and nitrate concentrations increased with depth (Supplementary Figure 1 and Supplementary material 4). Overall, phosphate concentrations ranged from 0.04 to  $1.04 \mu\text{mol L}^{-1}$ , silicate concentrations ranged from 0.20 to  $12.7 \mu\text{mol L}^{-1}$ , nitrate ranged from 0.00 to  $15.3 \mu\text{mol L}^{-1}$ , and nitrite ranged from 0.01 to  $0.35 \mu\text{mol L}^{-1}$  (Supplementary Figure 1 and Supplementary material 4). Phosphate concentrations were highest in the deepest samples of stations P6 and P7. The highest nitrate values were found in spring, with elevated concentrations throughout the water column (Supplementary Figure 1 and Supplementary material 4). At the same time, nitrite concentrations were low at all stations, never exceeding  $0.02 \mu\text{mol L}^{-1}$  (Supplementary Figure 1 and Supplementary material 4) but were still significant drivers for the community composition ( $p = 0.034$  surface;  $p = 0.024$  sub-seasurface; Figure 2). Chlorophyll *a* values were highest in the surface layers during spring, reaching  $3.17 \mu\text{g L}^{-1}$  at 30 m at P6 and even  $4.25 \mu\text{g L}^{-1}$  at 90 m at P7 (Supplementary Figure 1 and Supplementary material 4). The concentrations were low during summer, lower in early winter, and lowest concentrations were measured during late winter, when Chl *a* concentrations never exceeded  $0.02 \mu\text{g L}^{-1}$  (Supplementary Figure 1 and Supplementary material 4).

### 3.2. Bacterial and archaeal cell numbers

The bacterial and archaeal cell numbers were generally higher in surface waters with an average of  $2.9 \times 10^5 \pm 5.1 \times 10^4$  cells  $\text{ml}^{-1}$  than in the sub-seasurface with an average of  $1.4 \times 10^5 \pm 1.4 \times 10^4$  cells  $\text{ml}^{-1}$  (Supplementary Figure 1). Lowest cell abundances were found in the deepest samples at stations P6 and P7, which significantly ( $p = 0.001$ ) separated these samples from the rest of the sub-seasurface samples in the RDA (Figure 2; Supplementary Figure 1). They were overall highest during summer, especially in surface waters reaching  $2.3 \times 10^6$  cells  $\text{ml}^{-1}$  at 10 m depth at station P5 (Supplementary Figure 1). The cell abundance in surface waters

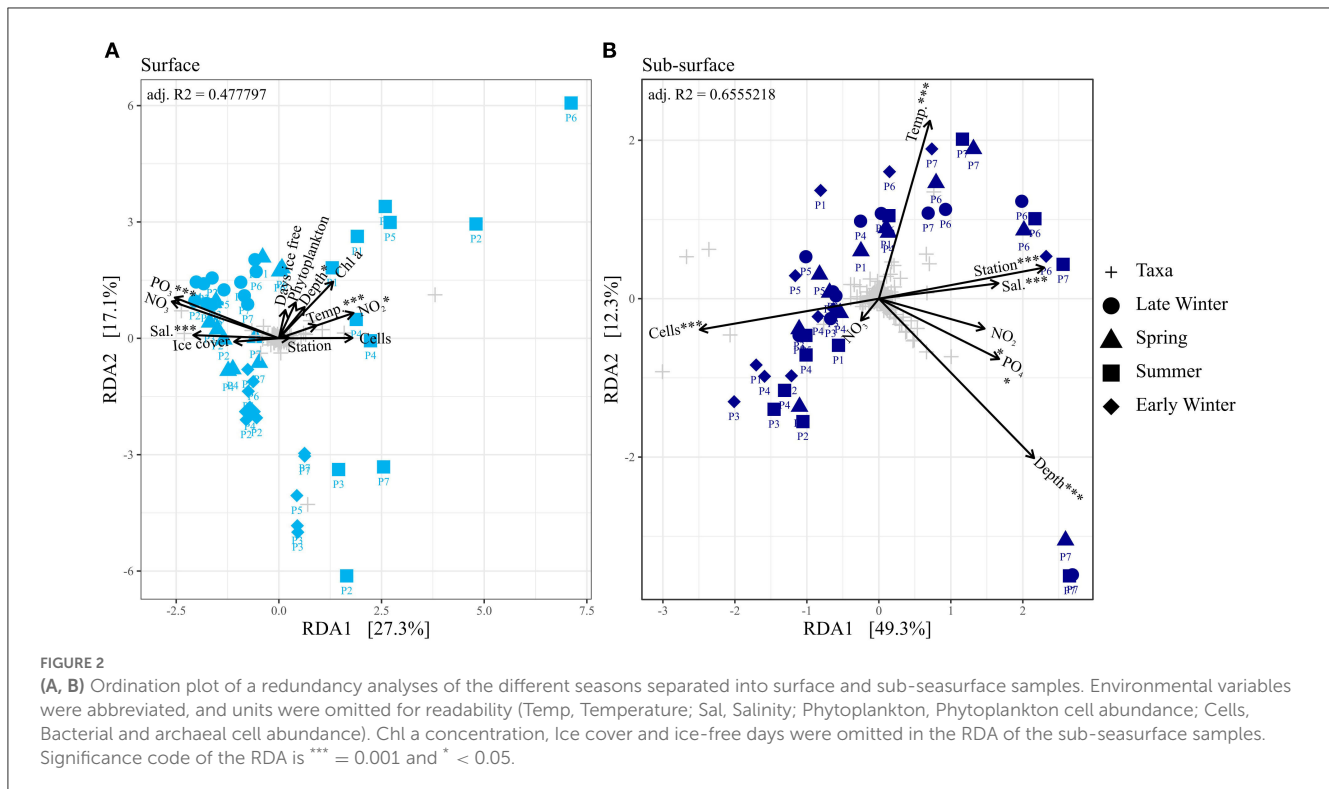
was lower in early winter, at a minimum in late winter, and higher again in spring (Supplementary Figure 1). These changes were more prominent in the surface waters, with cell numbers being more stable in the sub-seasurface (Supplementary Figure 1 and Supplementary material 4).

### 3.3. Bacterial and archaeal community composition

Bacterial and archaeal communities from surface and sub-seasurface waters were markedly different in spring, summer, and early winter, but relatively similar in late winter. For the surface samples, the season was the most prominent factor differentiating between the samples, while for sub-seasurface samples, the location accounted for the most differences (Figure 2). The bacterial community was dominated by *Alphaproteobacteria* and *Gammaproteobacteria* with  $55 \pm 14$  and  $44 \pm 7\%$  combined *Proteobacteria* relative abundance in the surface and sub-seasurface (Figure 3). *Bacteroidia* were second with  $14 \pm 17$  and  $4 \pm 5\%$ . These were complemented by members of the SAR324 clade, *Verrucomicrobiota*, *Nitrospinota*, *Marinimicrobia*, *Planctomycetota*, and *Chloroflexi*, which all were more abundant in sub-seasurface waters than at the surface. These phyla accounted for  $\sim 74\%$  of the community and were complemented by the archaeal phyla *Crenarchaea* and *Thermoplasmata* which together accounted for  $\sim 24\%$ . Both archaeal phyla were more abundant in sub-seasurface waters with  $22 \pm 4$  and  $6 \pm 3\%$ , than at the surface with  $17 \pm 11$  and  $3 \pm 2\%$ . In general, the sub-seasurface community was relatively stable throughout all four seasons, while the surface layer showed distinct changes in the bacterial and archaeal communities (Figure 3).

At the surface, *Nitrosphaeria*, specifically *Cand. Nitrosopumilus*, accounted for the most prominent changes over the four seasons (Figure 3). While *Cand. Nitrosopumilus* was dominant during late winter and spring with  $24 \pm 6\%$ , the relative abundance was  $<0.2\%$  during summer, before increasing again to  $14 \pm 8\%$  during early winter, but with lower abundance at stations P3, P5, and P7 ( $\sim 6\%$ , Figure 4). This pattern is closely mirrored by *Nitrospinia*, which co-occurred with *Cand. Nitrosopumilus* (Figure 3). Within the *Nitrospinia*, members of the LS-NOB clade were dominant with  $5 \pm 1\%$ ,  $1 \pm 1\%$ ,  $>0.01\%$ , and  $2 \pm 1\%$  relative abundance during late winter, spring, summer, and early winter, respectively (Figure 4).

*Bacteroidia* showed opposite patterns to *Cand. Nitrosopumilus* by being low in late winter ( $2 \pm 1\%$ ), increasing during spring ( $11 \pm 8\%$ ), peaking at  $37 \pm 21\%$  in summer, before decreasing again to  $7 \pm 3\%$  in early winter (Figure 3). Among the *Bacteroidia*, members of the NS9 group were the most constant with average relative abundances between 1% in late winter and 4% in spring (Figure 4). All other dominant *Bacteroidia* were below 0.5% relative abundance during late winter, spring, and early winter, except for *Polaribacter* which were elevated at stations P1, P4, and P6 during spring (1%, 3%, and 10%; Figure 4). During summer, all these groups became more dominant. Especially *Polaribacter*, with an average abundance of 17% in surface waters, was the second most abundant genus in the dataset. At station P6, *Polaribacter* made up



72% of the community at this time (Figure 4). Similarly, *Formosa*, *Ulvibacter*, *Flavobacteriaceae*, and members of the NS9 clade were higher during summer but showed differences between different stations (Figure 4).

Similar dynamics with different taxa being abundant at different stations were found for *Gammaproteobacteria*. Overall, *Gammaproteobacteria* had the lowest abundance during late winter, were more abundant in spring, peaked in summer, and were less abundant again in early winter ( $13 \pm 2\%$ ,  $18 \pm 7\%$ ,  $30 \pm 8\%$ , and  $17 \pm 3\%$ ; Figure 3). Within the *Gammaproteobacteria*, members of the SUP05 clade were most abundant, although mostly in sub-seasurface waters, where the taxon accounted for more than 5% of the total community (Figure 4). In surface waters, *Nitrincolaceae*, *Pseudohongiella*, and members of the SAR86 and SAR92 clades were the most dominant gammaproteobacteria taxa (Figure 4). In this study, *Pseudohongiella* and members of the SAR86 clade were relatively stable throughout the seasons at  $1$  and  $2 \pm 1\%$ , whereas *Nitrincolaceae* and members of the SAR92 and OM60(NOR5) clades varied more, all of them peaking during summer ( $9 \pm 6\%$ ,  $7 \pm 3\%$ , and  $4 \pm 4\%$ ; Figure 4). The standard deviation is the result of stations being highly variable during summer, when *Nitrincolaceae* were most abundant at P2, P5, and P7, members of the SAR92 clade at stations P1, P4, P5, and P7, and members of the OM60(NOR5) clade at P1, P4, and P5 (Figure 4). *Colwellia* was relatively abundant at 10 m depth at station P6 with 6% but was otherwise low (Figure 4).

*Alphaproteobacteria* was the most abundant class overall with  $30 \pm 3\%$ ,  $34 \pm 8\%$ , and  $30 \pm 19\%$  during late winter, spring, and summer, respectively, and higher during early winter with  $49 \pm 8\%$  (Figure 3). The most dominant taxa within the *Alphaproteobacteria* belonged to the SAR11 group, being members of the SAR11 Clades

I, Ib, II, and an unspecified SAR11 clade. While the latter three clades were stable with  $2 \pm 1\%$ ,  $6 \pm 3\%$ , and  $3 \pm 1\%$  during late winter, spring, and early winter, all were lower than 1% during summer (Figure 4). Members of the SAR11 Clade I were low during late winter and during spring with  $15 \pm 2\%$  and  $19 \pm 5\%$ , but very abundant, although with high variability between stations, during summer (e.g., 51%, 37%, and 45% at stations P2, P3, and P7). The highest relative abundance was found during early winter at  $33 \pm 9\%$  (Figure 4). A single peak of *Amylibacter* (previously NAC11-7 clade) was found with 6% at P1 during summer (Figure 4).

Among the *Verrucomicrobiae*, the Arctic97B-4 marine group dominated, being stable  $\sim 3\%$  in sub-seasurface waters, and 2% at the surface during late winter, but below the detection limit during summer (Figure 4). In this study, *Lentimonas* and *Luteolibacter* were more abundant in the sub-seasurface but also reached 5 and 4% in surface waters at stations P4 and P1 (Figure 4). These classes were complemented by members of the SAR202 and SAR324 clades, *Marinimicrobia*, and Marine Group II archaea of the *Thermoplasmata*, all of which were abundant in sub-seasurface but lower than 0.1% in surface waters during summer (Figures 3, 4).

### 3.4. Inferred metabolic potential of the bacterial and archaeal community

Using PiCRUST2, CAZymes and marker genes for nitrogen-, sulfur-, and methane metabolism, as well as photosynthesis, were inferred from genomes of closely related strains deposited in the NCBI database. Photosynthesis marker genes, *soxB*, *napA*, *hzsA*, and *mmoX* were not detected, while the abundance of

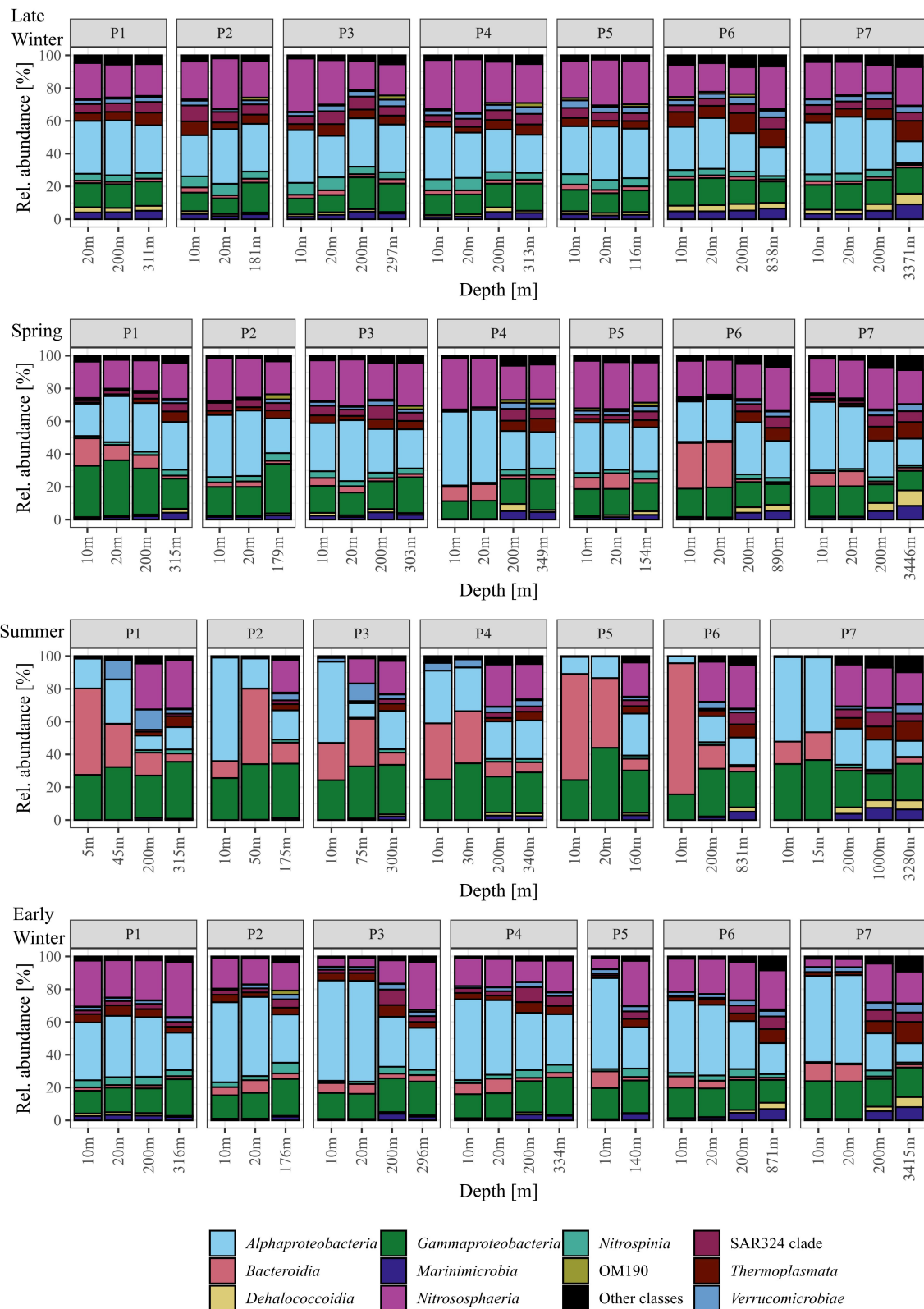


**FIGURE 3**  
 Relative abundance of the most abundant classes detected using 16S rRNA gene sequencing. Classes under 1% mean relative abundance are summed as "Other classes".

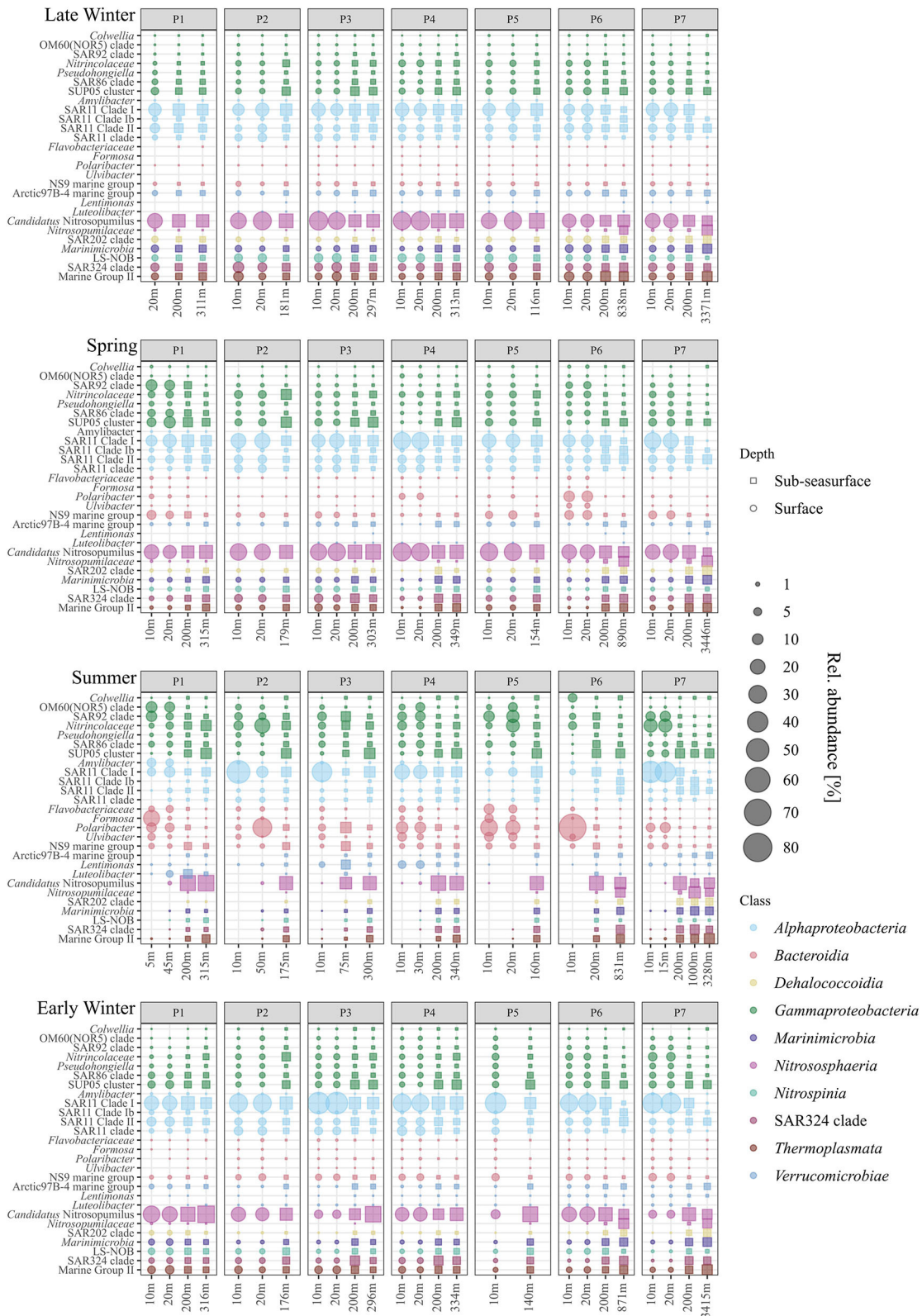


**FIGURE 4** Relative abundance of the most abundant genera per class (color coded) for surface (●) and sub-seasurface (■) waters of the stations P1 to P7 for 2021 (late winter, spring) and 2019 (summer, early winter).

marker genes for methane and sulfur metabolisms was low (*mcrA* and *dsrA*) or showed constant abundance among the samples (*cysH* and *aprA*). Genes for nitrogen metabolisms and CAZymes showed similar abundance in sub-seasurface waters throughout the samples and are therefore not shown. Surface samples were summed by the gene for each season as a conservative approach to investigate the inferred genes. Genes for nitrogen fixation (*nifH*), nitrate reduction to ammonium (*nrfA*), and denitrification (*narB*, *norB*, and *nosZ*) were low, except for *narB* with 0.14% relative sequence abundance during summer, mostly affiliated to *Bacteroidia* (Figure 5). The most abundant genes were related to nitrification (*amoA-pmoA*) and denitrification (*nirS/nirK*), and were affiliated to *Nitrospina*, *Nitrosphaeria*, mainly LS-NOB, and *Cand. Nitrosopumilus* and *Nitrosopumilaceae*, as well as *Gammaproteobacteria* (Figure 5). These genes were abundant during late winter and spring (0.6 and 1.4%, and 0.6 and 1.3%, for nitrification and denitrification, respectively; Figure 5). The abundance was <0.1% during summer and higher again to 0.4% and 0.8% in early winter (Figure 5). Most *amoA-pmoA* genes are affiliated with taxa known to perform nitrification. Hence, we assume that the gene is mostly the ammonia monooxygenase coding *amoA* involved in nitrification. However, methanotrophic taxa, such as *Methyloprofundus*, were also found, implying that *pmoA* genes involved in methanotrophy are included in small amounts. Since these abundances are approximately two orders of magnitude smaller than the abundance of *amoA*, we here refer to both genes as *amoA*.

Within the groups of CAZymes, only glycosyl hydrolases and glycosyl transferases were high and showed distinct changes in abundance. Glycosyl transferases, mostly affiliated with *Alphaproteobacteria*, *Gammaproteobacteria*, *Bacteroidia*, and many less abundant classes, were high during all quarters of the year, but were higher during late winter and spring (~8%) as compared to 6.7% during summer and early winter (Figure 5). Glycosyl hydrolases, affiliated to *Alphaproteobacteria*, *Gammaproteobacteria*, *Bacteroidia*, *Verrucomicrobia*, and many less abundant classes, were lowest in early and late winter with 3.9 and 3.26%, but higher in spring and summer with 4.22, and 8.02% (Figure 5).

## 4. Discussion

During the Nansen Legacy project, early winter and summer were sampled in 2019, while late winter and spring were sampled in 2021. The communities representing early and late winter are relatively similar despite being sampled more than 1 year apart. In addition, the summers in 2019 and 2021 were relatively similar in environmental conditions as well as the bacterial and archaeal communities (Thiele et al., 2023). This is further supported by the occurrence and dominance of identical ASVs of *Cand. Nitrosopumilus*, *Polaribacter*, and the main ASV of SAR11 Clade 1a, the most dominant taxa, in all samples. Therefore, we consider this dataset as a useful representation of major seasonal variations in the bacterial and archaeal community of this marine Arctic area.

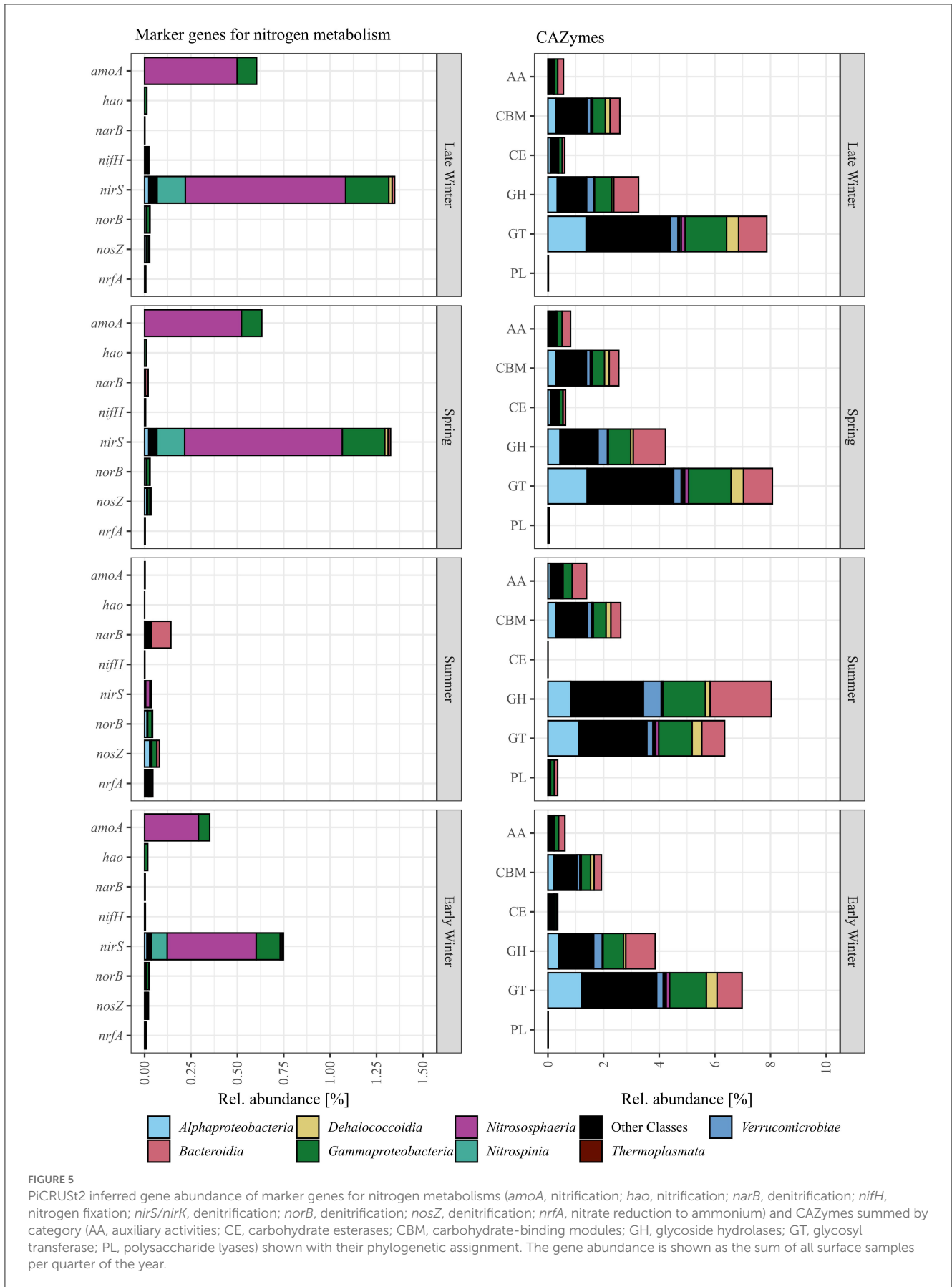
Except during late winter, the bacterial and archaeal communities in surface and sub-seasurface samples were different. In the sub-seasurface, the main differentiating factors

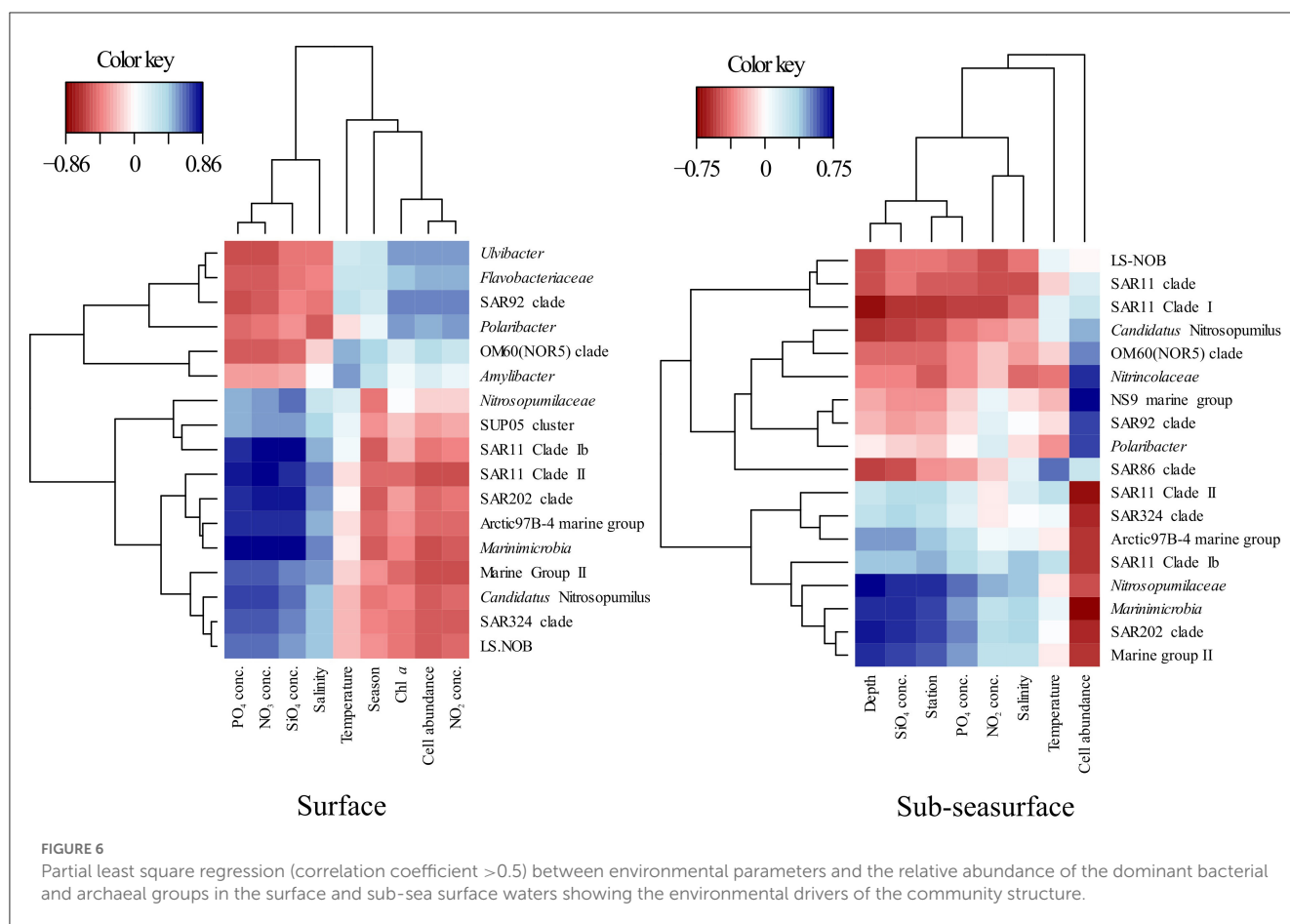
between samples were the location of the station, salinity, depth, temperature, phosphate and nitrite concentrations, and cell abundance, with P6 and P7 being the most different from other stations. These stations are deeper and have different water bodies in the deep waters, which explains the differences in temperature and salinity, as well as the higher phosphate and nitrite values. Generally, the abundance of bacterial and archaeal cells decreases with depth in the ocean thus explaining the lower cell numbers at the deep stations. The main environmental variables correlating with the sub-seasurface main bacterial and archaeal taxa, besides stations and depth, were higher phosphate and nitrite concentrations, lower cell abundance, temperatures, and higher salinity (Figure 6). However, the communities showed much less variation between the different seasons than in the surface waters. The community in the sub-seasurface samples was dominated by *Cand. Nitrosopumilus*, members of the SAR11 clades, *Marinimicrobia*, members of the SAR324 clade, and the LS-NOB clade within the *Thermoplasmata*. Similar communities have been found at different times in areas around Svalbard thus implying that these taxa broadly resemble the bacterial and archaeal community of sub-seasurface Arctic waters (Wilson et al., 2017; Müller et al., 2018; de Sousa et al., 2019).

In surface waters, cell numbers were low from late winter to spring, were highest in summer, and decreased again toward early winter, indicating a seasonality of the bacterial and archaeal community. This was confirmed by partial least square regression analyses determining the season, the correlated Chl *a* and nitrite concentrations, and cell abundance, as the main driving factors of the surface community composition (Figure 6). The surface water undergoes seasonal changes with constant daylight and higher temperatures in summer leading to ice melt and consequently slightly lower surface water salinity. At stations P1, P6, and P7, these changes could be an indicator of the influx of Atlantic waters into the Arctic by the West Spitsbergen Current at these stations (Loeng, 1991; Lind and Ingvaldsen, 2012; Asbjørnsen et al., 2020). However, following the “everything is everywhere”-hypothesis (O'Malley, 2008), large changes in the bacterial and archaeal community due to waters with only slightly different environmental conditions are unlikely. Secondary effects, such as the transport of phytoplankton blooms with the incoming waters, however, could be a factor for changes in the community composition (Oziel et al., 2020).

### 4.1. Spring

The environmental conditions during April/May 2021 were characterized by the highest concentrations of nitrate and Chl *a* in the waters. While the high nitrate concentration is a result of vertical mixing and, potentially, nitrification in surface waters during winter, the onset of the phytoplankton spring bloom in April and May provides carbon and energy to the whole Arctic marine ecosystem (Degerlund and Eilertsen, 2010; Assmy et al., 2017), including bacterial and archaeal communities (Teeling et al., 2012, 2016). This leads to a succession, mostly driven by bacterial groups specialized for carbon utilization, such as *Gammaproteobacteria* and *Bacteroidia*, hence explaining the higher abundance of these





groups in the spring. Members of the SAR92 clade, *Polaribacter*, and members of the NS9 clade had high abundances during spring, marking the onset of the succession. Members of the SAR92 clade were found as early responders to an Antarctic phytoplankton bloom (Liu et al., 2020), and *Polaribacter* has globally been found in co-occurrence with phytoplankton blooms (Gomez-Pereira et al., 2010; Thiele et al., 2012, 2015; Xing et al., 2015; Teeling et al., 2016). The NS9 clade has, however, not been found to correlate with phytoplankton blooms in polar environments.

## 4.2. Summer

The summer situation is reflected by the communities found during a late phytoplankton bloom situation (Thiele et al., 2023). In this study, *Nitrincolaceae* (formerly *Oceanospirillaceae*), members of the SAR92 and OM60(NOR5) clades were most abundant among the *Gammaproteobacteria*, while *Polaribacter*, *Formosa*, *Ulvibacter*, and *Flavobacteriaceae* ASVs were abundant members of the *Bacteroidia*. The abundance of these two classes indicates waters with elevated concentrations of phytoplankton-derived carbon sources (Simon et al., 1999; Puddu et al., 2003; Gomez-Pereira et al., 2010; Teeling et al., 2012, 2016; Thiele et al., 2012). *Nitrincolaceae* are known for high diversity in carbon utilization metabolisms and to rapidly respond to increased carbon availability. The group has been found in phytoplankton blooms

in Antarctica, the Arctic, and Arctic sea ice (Mori et al., 2019; Liu et al., 2020; Mönnich et al., 2020; Park et al., 2020; Wietz et al., 2021; Thiele et al., 2022). SAR92 clade members remained active in blooms, and members of the OM60(NOR5) clade have been found to correlate with phytoplankton blooms (Yang et al., 2015). In addition, a similar community of *Bacteroidia* consisting of *Polaribacter*, *Formosa*, NS9 clade, and further unidentified *Flavobacteriaceae* ASVs have been found in a spring–summer bloom in the Fram Strait west of Svalbard (Wietz et al., 2021). Generally, *Bacteroidia* co-occur in abundance with phytoplankton blooms, exploiting the derived carbon sources due to their multitude of carbon degradation pathways and carbohydrate-active enzyme content (Gomez-Pereira et al., 2010; Reintjes et al., 2019, 2020). Interestingly, a single peak of the *Amylibacter*, a taxon also found during summer to fall transitions west of Svalbard (Wietz et al., 2021), was found at station P1 indicating that this station might be in a later stage of the succession than the other stations, which is supported by lower Chl *a* values. Generally, the stations showed higher variability during summer, pointing toward different bloom stages, potentially due to ice coverage-mediated variability in the onset and strength of the spring phytoplankton bloom (Hunt et al., 2013; Silva et al., 2021). As the bloom progresses, different carbon sources are available, thus defining the nutritional habitat of the station and consequently determining the diversity and community structure of the bacterial and archaeal community (Teeling et al., 2012, 2016). This is supported by

the higher abundance of GH genes during summer, indicating that species with more CAZyme coding genes were abundant during summer. CAZymes, and specifically glycoside hydrolases are enzymes involved in the degradation of carbohydrates. GHs are a widespread group targeting glycosidic bonds of substrates ranging from monosaccharides to polysaccharides and complex sugar components, e.g., glucans, fucans, mannans, or cellulose (Teeling et al., 2016). By that, the occurrence of different GHs can give hints toward the carbohydrate preference of the different taxa, thus explaining the succession within the bacterial and archaeal community. However, since the inferences made by PiCRUST2 should only be used as indications, we have to refrain from detailed analyses of the different CAZyme groups.

Interestingly, *Cand. Nitrosopumilus* were substantially lower in surface waters during summer, although being abundant in the sub-seasurface throughout the year, and in surface samples during winter and spring. The same pattern has been found previously in Arctic water and ice and is attributed to the photoinhibition of ammonia oxidation (Collins et al., 2010; Grzymalski et al., 2012; Wilson et al., 2017; Müller et al., 2018; de Sousa et al., 2019; Thiele et al., 2022).

### 4.3. Early and late winter

The transition from summer to winter, including fall was not fully covered by our sampling, therefore it remains speculative if a second phytoplankton bloom occurred and provided additional carbon sources to the microbial loop. Such fall blooms have previously been reported for the southern Barents Sea (Ardyna et al., 2014; Silva et al., 2021). In early winter 2019, the bacterial and archaeal community had transitioned back to a “winter state” with a low abundance of *Bacteroidia* and *Gammaproteobacteria* and a high abundance of *Alphaproteobacteria*. The decrease of *Bacteroidia* and *Gammaproteobacteria* implies that the succession based on phytoplankton-derived carbon was over and that the remaining carbon sources in the surface waters did not provide favorable conditions for these classes. Thus, *Nitrospiraceae*, together with members of the SAR86 and SUP05 clades, were the most dominant *Gammaproteobacteria*, all of which have been found in rather oligotrophic/winter communities in polar environments (Thiele et al., 2012, 2022; Wietz et al., 2021). Members of the SAR11 clade became dominant, possibly due to a decrease of other groups, as SAR11 clade members dominate the “base community” in marine and specifically polar waters (Morris et al., 2002; Schattner et al., 2009; Thiele et al., 2012; Wilson et al., 2017; Wietz et al., 2021). In addition, *Cand. Nitrosopumilus* showed high abundance in the surface waters of some stations.

In late winter, *Cand. Nitrosopumilus* and members of the SAR11 clade were the most abundant taxa, and the surface layer closely resembled the sub-seasurface waters, with *Marinimicrobia*, members of the SAR202 and SAR324 clades, members of the Arctic97B-4 marine group, and the LS-NOB clade present at all depths, thus representing the winter community (Wilson et al., 2017; Müller et al., 2018). The co-occurrence of *Cand. Nitrosopumilus*, oxidizing ammonia to nitrite, and members of the LS-NOB clade (*Nitrospina*) potentially completing the nitrification process, hints toward a chemoautotrophic community (Könneke

et al., 2005; Luecker et al., 2013; Reji et al., 2019; Wietz et al., 2021; Rasmussen and Francis, 2022). This community oxidizes ammonia residuals derived from the decay of the spring/summer phytoplankton bloom, thus contributing to the replenishment of the nitrate pool toward spring. The high abundance of *amoA* genes during late winter and spring, which are affiliated with *Cand. Nitrosopumilus*, *Nitrosopumilaceae*, and members of the LS-NOB clade, supports this hypothesis. However, the abundance of *nirS/nirK* genes affiliated to *Cand. Nitrosopumilus*, *Nitrospina*, and *Gammaproteobacteria* indicate a truncated form of denitrification, as full denitrification would require anoxic conditions, and the respective genes were not found. Hence, only the first two steps of denitrification might be conducted (Graf et al., 2014).

In conclusion, we are here presenting the bacterial and archaeal community of spring, summer, and early and late winter, sampled over a transect covering the northern Barents Sea east of Svalbard and into the Arctic Ocean. A shift in the community occurred from a winter state dominated by members of the SAR11 clade and a community of nitrifiers, namely *Cand. Nitrosopumilus* and LS-NOB (*Nitrospina*), to spring and summer, with a succession of carbon-utilizing *Gammaproteobacteria* and *Bacteroidia*, back to an early winter state, with the re-establishment of ammonium oxidizers, and potential prevalence of chemoautotrophic metabolisms. The overarching Pattern observed in our year-round sampling from the northern Barents sea resembles findings from an automated sampler in the Fram Strait west of Svalbard, where a similar shift of metabolisms was observed, although partly by different taxa (Wietz et al., 2021). Our study corroborates that spring and summer carbon cycling and winter nitrogen cycling are important processes driving the microbial ecology of Arctic marine ecosystems, and although annual variations are to be expected, it provides a baseline for future study on these processes in response to the effects of climate change. Specifically, sea ice coverage and the correlated variability of the phytoplankton bloom timing and strength might become a factor for the bacterial and archaeal community and thereby carbon cycling in the Northern Barents Sea.

### Data availability statement

The datasets presented in this study can be found in online repositories. The names of the repository/repositories and accession number(s) can be found in the article/Supplementary material.

### Author contributions

STh analyzed the sequences and wrote the manuscript. STho, KS, EP, and OM conducted the laboratory preparations. AV, GB, and OM commented extensively on the manuscript. All authors contributed in the writing process.

### Funding

This study was funded by the Research Council of Norway through the project The Nansen Legacy (RCN # 276730).

## Acknowledgments

We would like to thank the captain and crews of the RV Kronprins Haakon, as well as the Leader of the RF3 of The Nansen Legacy, and all the project members that collected the data and helped obtain and process the samples.

## Conflict of interest

The authors declare that the research was conducted in the absence of any commercial or financial relationships that could be construed as a potential conflict of interest.

## Publisher's note

All claims expressed in this article are solely those of the authors and do not necessarily represent those of their affiliated organizations, or those of the publisher, the editors and the reviewers. Any product that may be evaluated in this article, or claim that may be made by its manufacturer, is not guaranteed or endorsed by the publisher.

## References

- Alonso-Sáez, L., Waller, A. S., Mende, D. R., Bakker, K., Farnelid, H., Yager, P. L., et al. (2012). Role for urea in nitrification by polar marine Archaea. *Proc. Natl. Acad. Sci. U.S.A.* 109, 17989–17994. doi: 10.1073/pnas.1201914109
- Apprill, A., McNally, S., Parsons, R., and Weber, L. (2015). Minor revision to V4 region SSU rRNA 806R gene primer greatly increases detection of SAR11 bacterioplankton. *Aquat. Microb. Ecol.* 75, 129–137. doi: 10.3354/ame01753
- Ardyna, M., Babin, M., Gosselin, M., Devred, E., Rainville, L., Tremblay, J.-É., et al. (2014). Recent Arctic Ocean sea ice loss triggers novel fall phytoplankton blooms. *Geophys. Res. Lett.* 41, 6207–6212. doi: 10.1002/2014GL061047
- Ardyna, M., Mundy, C. J., Mayot, N., Matthes, L. C., Oziel, L., Horvat, C., et al. (2020). Under-ice phytoplankton blooms: shedding light on the “invisible” part of arctic primary production. *Front. Mar. Sci.* 7, 608032. doi: 10.3389/fmars.2020.608032
- Asbjørnsen, H., Årthun, M., Skagseth, Ø., and Eldevik, T. (2020). Mechanisms underlying recent Arctic atlantification. *Geophys. Res. Lett.* 47, e2020GL088036. doi: 10.1029/2020GL088036
- Assmy, P., Fernández-Méndez, M., Duarte, P., Meyer, A., Randelhoff, A., Mundy, C. J., et al. (2017). Leads in Arctic pack ice enable early phytoplankton blooms below snow-covered sea ice. *Sci. Rep.* 7, 40850. doi: 10.1038/srep40850
- Brussaard, C. P. D. (2004). Optimization of procedures for counting viruses by flow cytometry. *Appl. Environ. Microbiol.* 70, 1506–1513. doi: 10.1128/AEM.70.3.1506-1513.2004
- Callahan, B. J., McMurdie, P. J., Rosen, M. J., Han, A. W., Johnson, A. J. A., Holmes, S. P., et al. (2016). DADA2: high-resolution sample inference from Illumina amplicon data. *Nat. Methods* 13, 581–583. doi: 10.1038/nmeth.3869
- Chierici, M. (2021a). *Water Column Data on Dissolved Inorganic Nutrients (Nitrite, Nitrate, Phosphate and Silicic Acid) from the Nansen LEGACY Seasonal Cruise Q3, 2019706, with R.V. Kronprins Haakon, 5-27 August 2019.* doi: 10.21335/NMDC-1472517325
- Chierici, M. (2021b). *Water Column Data on Dissolved Inorganic Nutrients (Nitrite, Nitrate, Phosphate and Silicic Acid) from the Nansen LEGACY Seasonal Cruise Q4, 2019711, with R.V. Kronprins Haakon, 30 November-13 December 2019.* doi: 10.21335/NMDC-1629206101
- Collins, R. E., Rocap, G., and Deming, J. W. (2010). Persistence of bacterial and archaeal communities in sea ice through an Arctic winter. *Environ. Microbiol.* 12, 1828–1841. doi: 10.1111/j.1462-2920.2010.02179.x
- Connelly, T. L., Baer, S. E., Cooper, J. T., Bronk, D. A., and Wawrik, B. (2014). Urea uptake and carbon fixation by marine pelagic bacteria and archaea during the arctic summer and winter seasons. *Appl. Environ. Microbiol.* 80, 6013–6022. doi: 10.1128/AEM.01431-14
- de Sousa, A. G. G., Tomasino, M. P., Duarte, P., Fernández-Méndez, M., Assmy, P., Ribeiro, H., et al. (2019). Diversity and composition of pelagic prokaryotic and protist communities in a thin arctic sea-ice regime. *Microb. Ecol.* 78, 388–408. doi: 10.1007/s00248-018-01314-2
- Degerlund, M., and Eilertsen, H. C. (2010). Main species characteristics of phytoplankton spring blooms in NE Atlantic and Arctic Waters (68–80° N). *Estuaries Coasts* 33, 242–269. doi: 10.1007/s12237-009-9167-7
- Douglas, G. M., Maffei, V. J., Zaneveld, J. R., Yurgel, S. N., Brown, J. R., Taylor, C. M., et al. (2020). PICRUSt2 for prediction of metagenome functions. *Nat. Biotech.* 38, 685–688. doi: 10.1038/s41587-020-0548-6
- Gomez-Pereira, P. R., Fuchs, B. M., Alonso, C., Oliver, M. J., van Beusekom, J. E. E., Amann, R., et al. (2010). Distinct flavobacterial communities in contrasting water masses of the North Atlantic Ocean. *ISME J.* 4, 472–487. doi: 10.1038/ismej.2009.142
- Graf, D. R. H., Jones, C. M., and Hallin, S. (2014). Intergenomic comparisons highlight modularity of the denitrification pathway and underpin the importance of community structure for N<sub>2</sub>O emissions. *PLoS ONE* 9, e114118. doi: 10.1371/journal.pone.0114118
- Grüning, B., Dale, R., Sjödin, A., Chapman, B. A., Rowe, J., Tomkins-Tinch, C. H., et al. (2018). Bioconda: sustainable and comprehensive software distribution for the life sciences. *Nat. Methods* 15, 475–476. doi: 10.1038/s41592-018-0046-7
- Grzymalski, J. J., Riesenfeld, C. S., Williams, T. J., Dussaq, A. M., Ducklow, H., Erickson, M., et al. (2012). A metagenomic assessment of winter and summer bacterioplankton from Antarctica Peninsula coastal surface waters. *ISME J.* 6, 1901–1915. doi: 10.1038/ismej.2012.31
- Hodal, H., and Kristiansen, S. (2008). The importance of small-celled phytoplankton in spring blooms at the marginal ice zone in the northern Barents Sea. *Deep Sea Res. Pt. II* 55, 2176–2185. doi: 10.1016/j.dsr2.2008.05.012
- Hunt, G. L., Blanchard, A. L., Boveng, P., Dalpadado, P., Drinkwater, K. F., Eisner, L., et al. (2013). The barents and chukchi seas: comparison of two arctic shelf ecosystems. *J. Mar. Syst.* 109–110, 43–68. doi: 10.1016/j.jmarsys.2012.08.003

## Supplementary material

The Supplementary Material for this article can be found online at: <https://www.frontiersin.org/articles/10.3389/fmicb.2023.1213718/full#supplementary-material>

### SUPPLEMENTARY MATERIAL 1

Table of sequence counts and relative abundance [%] of ASVs after the removal of ASVs with total abundances <4. The samples are named with the time of the year (late winter, early winter, spring, and summer), station (P1–P7), and depth in meters, e.g., late winter\_P1\_0020 m.

### SUPPLEMENTARY MATERIAL 2

List of CAZymes used in this study.

### SUPPLEMENTARY MATERIAL 3

List of marker genes by metabolism used in this study.

### SUPPLEMENTARY MATERIAL 4

Table of environmental parameters measured at the different stations and depth.

### SUPPLEMENTARY FIGURE S1

Depth profiles of the environmental variables measured during late winter (□), spring (Δ), summer (○), and early winter (∇). Column one depicts the temperature (blue) and the salinity (red), column two depicts the concentrations of phosphate (turquoise), silicate (orange), nitrate (dark yellow), and nitrite (yellow), column three depicts the chlorophyll *a* concentration (green), and column four depicts the abundance of bacterial and archaeal cells (black). Missing values were interpolated when possible, using a simple mean of the value above and below in the depth profile.

- Ingvaldsen, R. B., Assmann, K. M., Primicerio, R., Fosshem, M., Polyakov, I. V., Dolgov, A. V., et al. (2021). Physical manifestations and ecological implications of Arctic Atlantification. *Nat. Rev. Earth Environ.* 2, 874–889. doi: 10.1038/s43017-021-00228-x
- Jones, E., Chierici, M., Hodal Lødemel, H., Møgster, J., and Fonnes, L. L. (2022a). *Water Column Data on Dissolved Inorganic Nutrients (Nitrite, Nitrate, Phosphate and Silicic Acid) from Process (P) Stations During the Nansen LEGACY Seasonal Cruise Q1, 2021/703, with R.V. Kronprins Haakon, 4-17 March 2021.* doi: 10.21335/NMDC-762320451
- Jones, E., Chierici, M., Hodal Lødemel, H., Møgster, J., and Fonnes, L. L. (2022b). *Water Column Data on Dissolved Inorganic Nutrients (Nitrite, Nitrate, Phosphate and Silicic Acid) from Process (P) Stations During the Nansen LEGACY Seasonal Cruise Q2, 2021/704, with R.V. Kronprins Haakon, 30 April - 18 May 2021.* doi: 10.21335/NMDC-487023368
- Könneke, M., and Bernhard, A. E. de la Torre, J. R., Walker, C. B., Waterbury, J. B., Stahl, D. A. (2005). Isolation of an autotrophic ammonia-oxidizing marine archaeon. *Nature* 437, 543–546. doi: 10.1038/nature03911
- Lin Pedersen, T. (2020). *patchwork: The Composer of Plots.* R package version 1.1.0. Available online at: <https://CRAN.R-project.org/package=patchwork> (accessed January 2023).
- Lind, S., and Ingvaldsen, R. B. (2012). Variability and impacts of Atlantic Water entering the Barents Sea from the north. *Deep-Sea Res. I: Oceanogr. Res. Pap.* 62, 70–88. doi: 10.1016/j.dsr.2011.12.007
- Liu, Y., Blain, S., Crispi, O., Rembauville, M., and Obernosterer, I. (2020). Seasonal dynamics of prokaryotes and their associations with diatoms in the Southern Ocean as revealed by an autonomous sampler. *Environ. Microbiol.* 22, 3968–3984. doi: 10.1111/1462-2920.15184
- Loeng, H. (1991). Features of the physical oceanographic conditions of the Barents Sea. *Polar Res.* 10, 5–18. doi: 10.3402/polar.v10i1.6723
- Luecker, S., Nowka, B., Rattai, T., Spieck, E., and Daims, H. (2013). The genome of *Nitrospina gracilis* illuminates the metabolism and evolution of the major marine nitrite oxidizer. *Front. Microbiol.* 4, 27. doi: 10.3389/fmicb.2013.00027
- Marie, D., Brussaard, C. P. D., Thyraug, R., Bratbak, G., and Vault, D. (1999). Enumeration of marine viruses in culture and natural samples by flow cytometry. *Appl. Environ. Microbiol.* 65, 45–52. doi: 10.1128/AEM.65.1.45-52.1999
- McMurdie, P. J., and Holmes, S. (2013). phyloseq: an R package for reproducible interactive analysis and graphics of microbiome census data. *PLoS ONE* 8, e61217. doi: 10.1371/journal.pone.0061217
- Mönnich, J., Tebben, J., Bergemann, J., Case, R., Wohlrab, S., Harder, T., et al. (2020). Niche-based assembly of bacterial consortia on the diatom *Thalassiosira rotula* is stable and reproducible. *ISME J.* 14, 1614–1625. doi: 10.1038/s41396-020-0631-5
- Mori, J. F., Chen, L.-X., Jessen, G. L., Rudderham, S. B., McBeth, J. M., Lindsay, M. B. J., et al. (2019). Putative mixotrophic nitrifying-denitrifying gammaproteobacteria implicated in nitrogen cycling within the ammonia/oxygen transition zone of an oil sands pit lake. *Front. Microbiol.* 10, 2435. doi: 10.3389/fmicb.2019.02435
- Morris, R. M., Rappe, M. S., Connon, S. A., Vergin, K. L., Siebold, W. A., Carlson, C. A., et al. (2002). SAR11 clade dominates ocean surface bacterioplankton communities. *Nature* 420, 806–810. doi: 10.1038/nature01240
- Müller, O., Wilson, B., Paulsen, M. L., Rumińska, A., Armo, H. R., Bratbak, G., et al. (2018). Spatiotemporal dynamics of ammonia-oxidizing thaumarchaeota in distinct arctic water masses. *Front. Microbiol.* 9, 24. doi: 10.3389/fmicb.2018.00024
- Oksanen, J., Blanchet, F. G., Friendly, M., Kindt, R., Legendre, P., McGlinn, D., et al. (2020). *vegan: Community Ecology Package.* R package version 2, 5–7. Available online at: <https://CRAN.R-project.org/package=vegan> (accessed January 2023).
- O'Malley, M. A. (2008). 'Everything is everywhere: but the environment selects': ubiquitous distribution and ecological determinism in microbial biogeography. *Stud. Hist. Philos. Biol. Biomed. Sci.* 39, 314–325. doi: 10.1016/j.shpsc.2008.06.005
- Oziel, L., Baudena, A., Ardyna, M., Massicotte, P., Randelhoff, A., Sallée, J.-B., et al. (2020). Faster Atlantic currents drive poleward expansion of temperate phytoplankton in the Arctic Ocean. *Nat. Commun.* 11, 1705. doi: 10.1038/s41467-020-15485-5
- Parada, A. E., Needham, D. M., and Fuhrman, J. A. (2016). Every base matters: assessing small subunit rRNA primers for marine microbiomes with mock communities, time series and global field samples. *Environ. Microbiol.* 18, 1403–1414. doi: 10.1111/1462-2920.13023
- Paradis, E., and Schliep, K. (2019). ape 5.0: an environment for modern phylogenetics and evolutionary analyses in R. *Bioinformatics* 35, 526–528. doi: 10.1093/bioinformatics/bty633
- Park, B. S., Lee, M., Shin, K., and Baek, S. H. (2020). Response of the bacterioplankton composition to inorganic nutrient loading and phytoplankton in southern Korean coastal waters: a mesocosm study. *Mar. Ecol.* 41, e12591. doi: 10.1111/maec.12591
- Price, M. N., Dehal, P. S., and Arkin, A. P. (2010). FastTree 2 – approximately maximum-likelihood trees for large alignments. *PLoS ONE* 5, e9490. doi: 10.1371/journal.pone.0009490
- Pruesse, E., Peplies, J., and Glöckner, F. O. (2012). SINA: accurate high-throughput multiple sequence alignment of ribosomal RNA genes. *Bioinformatics* 28, 1823–1829. doi: 10.1093/bioinformatics/bts252
- Puddu, A., Zoppini, A., Fazi, S., Rosati, M., Amalfitano, S., Magaletti, E., et al. (2003). Bacterial uptake of DOM released from P-limited phytoplankton. *FEMS Microbiol. Ecol.* 46, 257–268. doi: 10.1016/S0168-6496(03)00197-1
- Quast, C., Pruesse, E., Yilmaz, P., Gerken, J., Schweer, T., Yarza, P., et al. (2013). The SILVA ribosomal RNA gene database project: improved data processing and web-based tools. *Nucl. Acids Res.* 41, D590–D596. doi: 10.1093/nar/gks1219
- R Core Team (2021). *A Language and Environment for Statistical Computing.* Vienna: R Foundation for Statistical Computing. Available online at: <https://www.R-project.org/> (accessed January 2023).
- Rantanen, M., Karpechko, A. Y., Lipponen, A., Nordling, K., Hyvärinen, O., Ruosteenoja, K., et al. (2022). The Arctic has warmed nearly four times faster than the globe since 1979. *Commun. Earth Environ.* 3, 1–10. doi: 10.1038/s43247-022-00498-3
- Rasmussen, A. N., and Francis, C. A. (2022). Genome-resolved metagenomic insights into massive seasonal ammonia-oxidizing archaea blooms in San Francisco Bay. *mSystems* 7, e01270–21. doi: 10.1128/msystems.01270-21
- Reigstad, M., Wassmann, P., Wexels Riser, C., Øygarden, S., and Rey, F. (2002). Variations in hydrography, nutrients and chlorophyll a in the marginal ice-zone and the central Barents Sea. *J. Mar. Syst.* 38, 9–29. doi: 10.1016/S0924-7963(02)00167-7
- Reintjes, G., Arnosti, C., Fuchs, B., and Amann, R. (2019). Selfish, sharing and scavenging bacteria in the Atlantic Ocean: a biogeographical study of bacterial substrate utilisation. *ISME J.* 13, 1119–1132. doi: 10.1038/s41396-018-0326-3
- Reintjes, G., Fuchs, B. M., Scharfe, M., Wiltshire, K. H., Amann, R., Arnosti, C., et al. (2020). Short-term changes in polysaccharide utilization mechanisms of marine bacterioplankton during a spring phytoplankton bloom. *Environ. Microbiol.* 22, 1884–1900. doi: 10.1111/1462-2920.14971
- Reji, L., Tolar, B. B., Smith, J. M., Chavez, F. P., and Francis, C. A. (2019). Differential co-occurrence relationships shaping ecotype diversification within Thaumarchaeota populations in the coastal ocean water column. *ISME J.* 13, 1144–1158. doi: 10.1038/s41396-018-0311-x
- Rohart, F., Gautier, B., Singh, A., and Cao, K.-A. L. (2017). mixOmics: an R package for 'omics feature selection and multiple data integration. *PLoS Comput. Biol.* 13, 108597. doi: 10.1371/journal.pcbi.1005752
- Sakshaug, E. (2004). "Primary and secondary production in the Arctic Seas," in *The Organic Carbon Cycle in the Arctic Ocean*, eds. R. Stein, and R. W. MacDonald (Berlin: Springer), 57–81. doi: 10.1007/978-3-642-18912-8\_3
- Schattenhofer, M., Fuchs, B. M., Amann, R., Zubkov, M. V., Tarran, G. A., Perntaler, J., et al. (2009). Latitudinal distribution of prokaryotic picoplankton populations in the Atlantic Ocean. *Environ. Microbiol.* 11, 2078–2093. doi: 10.1111/j.1462-2920.2009.01929.x
- Silva, E., Counillon, F., Brajard, J., Korosov, A., Pettersson, L. H., Samuelsen, A., et al. (2021). Twenty-one years of phytoplankton bloom phenology in the Barents, Norwegian, and North Seas. *Front. Mar. Sci.* 8, 746327. doi: 10.3389/fmars.2021.746327
- Simon, M., Glöckner, F., and Amann, R. (1999). Different community structure and temperature optima of heterotrophic picoplankton in various regions of the Southern Ocean. *Aquat. Microb. Ecol.* 18, 275–284. doi: 10.3354/ame018275
- Smedsrud, L. H., Esau, I., Ingvaldsen, R. B., Eldevik, T., Haugan, P. M., Li, C., et al. (2013). The role of the Barents Sea in the Arctic climate system. *Rev. Geophys.* 51, 415–449. doi: 10.1002/rog.20017
- Ssekagiri, A., Sloan, W., and Ijaz, U. (2017). *microbiomeSeq: An R Package for Analysis of Microbial Communities in an Environmental Context.* doi: 10.13140/RG.2.2.17108.71047
- Steer, A., and Divine, D. (2023). *Sea Ice Concentrations in the Northern Barents Sea and the Area North of Svalbard at Nansen Legacy Stations During 2017–2021.*
- Sundfjord, A., Assmann, K. M., Lundesgaard, Ø., Renner, A. H. H., Lind, S., Ingvaldsen, R. B., et al. (2020). *Suggested Water Mass Definitions for the Central and Northern Barents Sea, and the Adjacent Nansen Basin: Workshop Report.* The Nansen Legacy Report Series. Tromsø: The Nansen Legacy. doi: 10.7557/nlrs.5707
- Teeling, H., Fuchs, B., Becher, D., Klockow, C., Gardebrecht, A., Bennis, C. M., et al. (2012). Substrate-controlled succession of marine bacterioplankton populations induced by a phytoplankton bloom. *Science* 336, 608–611. doi: 10.1126/science.1218344
- Teeling, H., Fuchs, B. M., Bennis, C. M., Krüger, K., Chafee, M., Kappelmann, L., et al. (2016). Recurring patterns in bacterioplankton dynamics during coastal spring algae blooms. *Elife* 5, e11888. doi: 10.7554/eLife.11888
- The Nansen Legacy (2021). *Sampling Protocols: The Nansen Legacy Report Series.* Tromsø: The Nansen Legacy. doi: 10.7557/nlrs.5793
- Thiele, S., Fuchs, B. M., Amann, R., and Iversen, M. H. (2015). Colonization in the photic zone and subsequent changes during sinking determine bacterial community composition in marine snow. *Appl. Environ. Microbiol.* 81, 1463–1471. doi: 10.1128/AEM.02570-14

- Thiele, S., Fuchs, B. M., Ramaiah, N., and Amann, R. (2012). Microbial community response during the iron fertilization experiment LOHAFEX. *Appl. Environ. Microbiol.* 78, 8803–8812. doi: 10.1128/AEM.01814-12
- Thiele, S., Storesund, J. E., Fernández-Méndez, M., Assmy, P., and Øvreås, L. (2022). A winter-to-summer transition of bacterial and archaeal communities in arctic sea ice. *Microorganisms* 10, 1618. doi: 10.3390/microorganisms10081618
- Thiele, S., Vader, A., Thomson, S., Saubrekka, K., Petelenz, E., Rief Armo, H., et al. (2023). The summer bacterial and archaeal community composition of the northern Barents Sea. *Prog. Oceanogr.* 215, 103054. doi: 10.1016/j.pocean.2023.103054
- Vihtakari, M. (2022). *Plot Data on Oceanographic Maps using ggplot2*. Available online at: <https://mikkovihtakari.github.io/ggOceanMaps/#citations-and-data-sources> (accessed October 6, 2022).
- Wassmann, P., Duarte, C. M., Agustí, S., and Sejr, M. K. (2011). Footprints of climate change in the Arctic marine ecosystem. *Glob. Chang. Biol.* 17, 1235–1249. doi: 10.1111/j.1365-2486.2010.02311.x
- Wickham, H. (2009). *ggplot2: Elegant Graphics for Data Analysis*. New York, NY: Springer. doi: 10.1007/978-0-387-98141-3
- Wickham, H. (2020). *forcats: Tools for Working with Categorical Variables (Factors)*. R package version 0.5.0. Available online at: <https://CRAN.R-project.org/package=forcats> (accessed January 2023).
- Wickham, H., Averick, M., Bryan, J., Chang, W., McGowan, L. D., François, R., et al. (2019). Welcome to the tidyverse. *J. Open Source Softw.* 4, 1686. doi: 10.21105/joss.01686
- Wickham, H., and Seidel, D. (2020). *scales: Scale Functions for Visualization*. R package version 1.1.1. Available online at: <https://CRAN.R-project.org/package=scales> (accessed January 2023).
- Wietz, M., Bienhold, C., Metfies, K., Torres-Valdés, S., von Appen, W.-J., Salter, I., et al. (2021). The polar night shift: seasonal dynamics and drivers of Arctic Ocean microbiomes revealed by autonomous sampling. *ISME Commun.* 1, 1–12. doi: 10.1038/s43705-021-00074-4
- Wilson, B., Müller, O., Nordmann, E.-L., Seuthe, L., Bratbak, G., Øvreås, L., et al. (2017). Changes in marine prokaryote composition with season and depth over an arctic polar year. *Front. Mar. Sci.* 4, 95. doi: 10.3389/fmars.2017.00095
- Xing, P., Hahnke, R. L., Unfried, F., Markert, S., Huang, S., Barbeyron, T., et al. (2015). Niches of two polysaccharide-degrading *Polaribacter* isolates from the North Sea during a spring diatom bloom. *ISME J.* 9, 1410–1422. doi: 10.1038/ismej.2014.225
- Yang, C., Li, Y., Zhou, B., Zhou, Y., Zheng, W., Tian, Y., et al. (2015). Illumina sequencing-based analysis of free-living bacterial community dynamics during an Akashiwo sanguine bloom in Xiamen sea, China. *Sci. Rep.* 5, 8476. doi: 10.1038/srep08476